Microstructure and corrosion behavior of Al-TiB$_2$/TiC composites processed by hot rolling

Jinfeng Nie[a,*], Fang Wang[a], Yuyao Chen[a], Qingzhong Mao[a], Huabing Yang[b], Zhiwei Song[a], Xiangfa Liu[b], Yonghao Zhao[a,*]

[a] Nano and Heterogeneous Materials Center, School of Materials Science and Engineering, Nanjing University of Science and Technology, Nanjing 210094, China
[b] Key Laboratory for Liquid–Solid Structural Evolution and Processing of Materials, Ministry of Education, Shandong University, Jinan 250061, China

ARTICLE INFO

ABSTRACT

The microstructure and corrosion behavior of Al-5 wt.% TiB$_2$/TiC composites after hot rolling treatment were investigated by scanning electron microscope, immersion tests, potentiodynamic polarization and electrochemical impedance spectroscopy (EIS) in 3.5 wt.% NaCl solution. The results show that corrosion of α-Al phase initiates at the interfaces between the matrix and the agglomeration clusters of TiB$_2$ and TiC particles. After hot rolling deformation, the dispersive distribution of reinforcement particles and the grain refinement of the Al matrix suppressed the rapid expansion of corrosion pits, which become smaller and shallower, indicating that the corrosion resistance of Al-TiB$_2$/TiC composites has been enhanced by hot rolling treatment.

Introduction

Aluminum matrix composites reinforced by ceramic particles have a wide application prospect in transportation, automobile and aircraft due to their excellent mechanical properties such as high modulus, high specific strength and et al. [1–3]. TiB$_2$ and TiC particles have been widely used as reinforcement particles, due to their unique properties such as low density, superior thermal and chemical stability, excellent wear resistance and high fracture toughness [4–8]. Many efforts have been made to fabricate Al-TiB$_2$/TiC composites. Zhu et al. [9] have attempted to fabricate the (α-Al$_2$O$_3$-TiB$_2$-TiC)/Al composites by using the exothermic dispersion synthesis route. Kim and Yu [10] fabricated TiC/Al composites using a combination of ball-milling and sheath rolling techniques. Generally, the liquid metallurgy route has attracted more attention because of its simplicity, low cost and mass production [11]. In-situ melt reaction is a one of favorable ways to obtain the Al-TiB$_2$/TiC composites, which allows the clearer interfaces between the matrix and particle reinforcements and better interfacial thermodynamic stability than those synthesized with exogenously formed process [12]. However, the reinforcement particles formed in the melt segregate at the grain boundaries seriously, which decrease the mechanical properties of the composites to some extent [13]. In order to enhance the properties of the composites, some plastic deformation processes such as rolling, equal channel angular pressing (ECAP), accumulative roll-bonding (ARB) and high-pressure torsion (HPT) have

been applied to optimize the microstructure and properties [14–17].

It is known that corrosion resistance of the Al based composites is also crucial in practical engineering application, which is decided by the microstructure of the Al matrix and distribution of the refinement particles. The effect of alumina particle size and content on the corrosion resistance of AA1070 aluminum in chloride/sulphate solution had been studied, which indicated that reduce the particle size will lead to lower corrosion rate [18]. Some studies have also been carried out to study the effect of deformation treatment on the corrosion resistance of Al alloys. Mustafa Abdulstaar [19] studied the corrosion behavior of ultrafine-grained (UFG) commercial pure aluminum Al 1050 processed by rotary swaging (RS) and the results showed that grain refinement led to marked improvement of the corrosion resistance. It was found that the corrosion resistance of aluminum alloys had been improved after ECAP treatment [20,21].

The corrosion behavior of metal matrix composites (MMC) fabricated by accumulative roll bonding (ARB) processes were investigated and the corrosion resistance became better with the increase of cycles [22,23]. Therefore, it has been proved that deformation treatment can improve the corrosion resistance of the alloys. However, there are limited reports about the influence of deformation on the corrosion performance of the Al-TiB$_2$/TiC composites.

In our previous work, the effect of ARB and hot rolling on the mechanical properties of Al-TiB$_2$/TiC composites have been studied [24,26], and both the distribution of particles and the mechanical
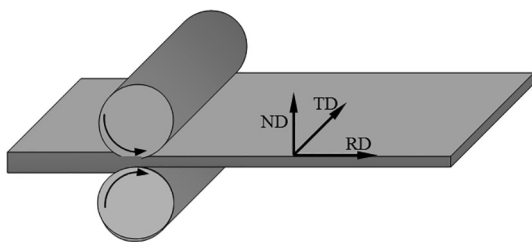
Fig. 1. Schematic illustration of the rolling process.

properties have been enhanced during the deformation process. Herein, the corrosion behavior of the composites after hot rolling treatment has been evaluated by gravimetric analysis, electrochemical impedance spectroscopy (EIS) and potentiodynamic polarization (PDC) measurements in 3.5 wt.% NaCl solution at room temperature. Besides, the corrosion mechanisms of the composites were also analyzed through the surface morphologies of the samples before and after corrosion tests.

Experimental procedures

Materials

An Al-5%TiB$_2$/TiC aluminum matrix composite was prepared by the direct melt reaction of Al-Ti and Al-B-C alloys and the reinforcement
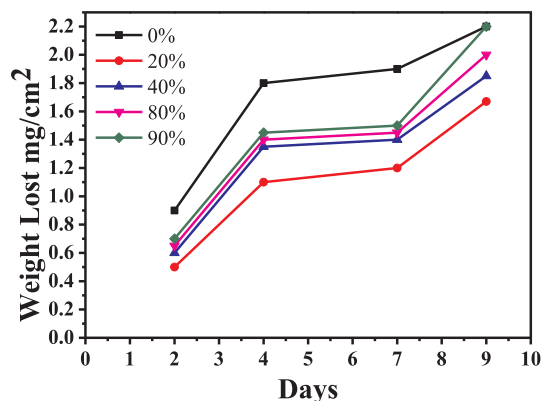

Fig. 3. Variation of the weight loss of Al-TiB$_2$/TiC composites with different rolling reduction as a function of duration time in 3.5 wt.% NaCl solution.

particles of TiB$_2$ and TiC were in-situ formed during the reaction. Subsequently, several plates of length 20 mm, width of 10 mm, and thickness of 10 mm were cut from the as-cast ingot of the composites for further hot rolling process. Fig. 1 is the schematic illustration of the hot rolling process to obtain the Al-TiB$_2$/TiC composite with the 20%, 40%, 80% and 90% reduction, and the specific details has been given in our previous work [24,26]. The composite plates were preheated at 300 °C for 5 min in a resistance furnace firstly, and then rolled on the
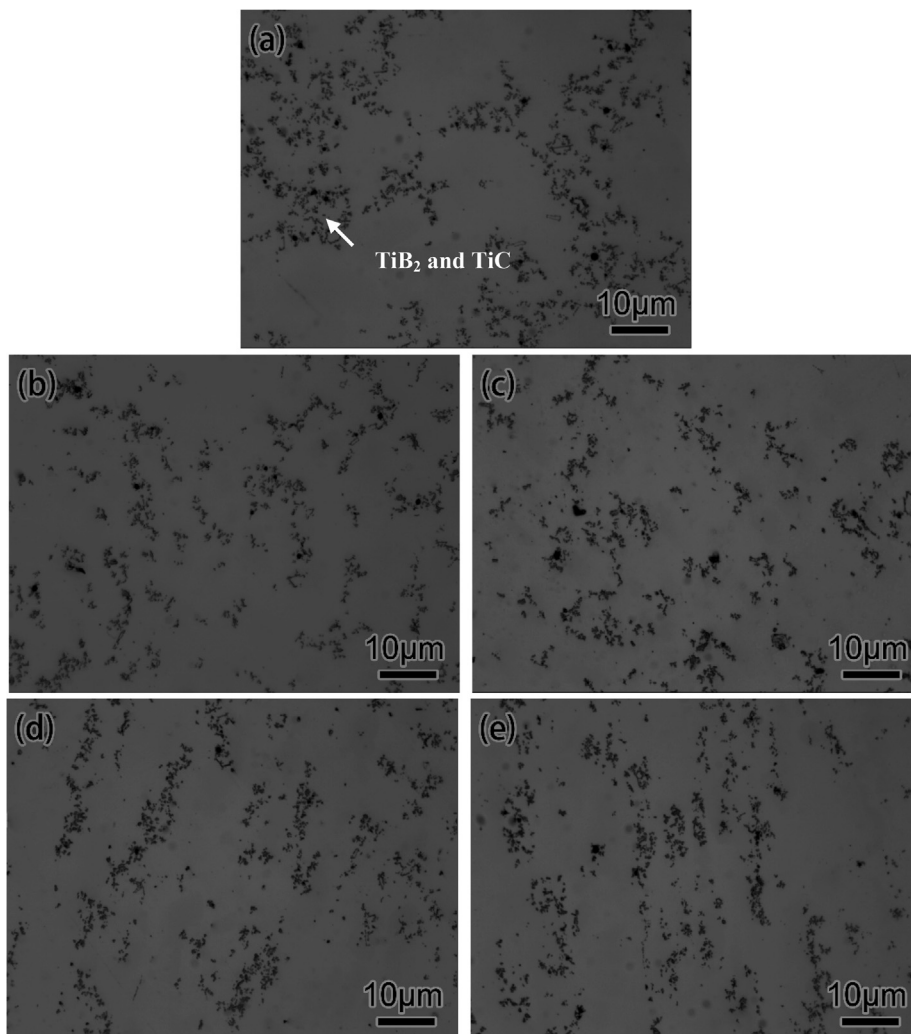

Fig. 2. Microstructures of the composites with different rolling reduction on the RD-TD plane: (a) as-cast; (b) 20%; (c) 40%; (d) 80%; (e) 90%.
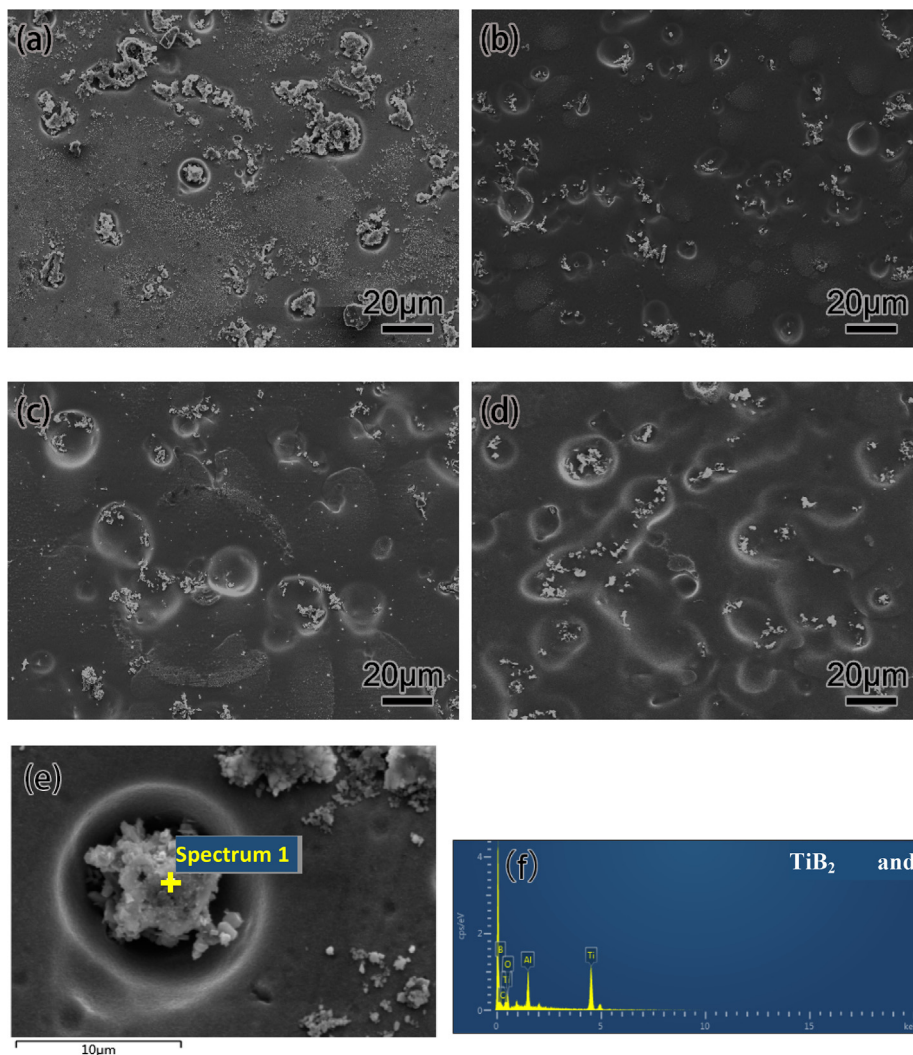
Fig. 4. SEM images of the corroded Al-TiB$_2$/TiC composites with 20% reduction immersed for different days and the EDS analysis after cleaned by CrO$_3$:H$_3$PO$_4$ (specific gravity 1.69): (a–d) immersed for 2, 4, 7 and 9 days; (e, f) EDS point analysis of the sample immersed for 2 days.
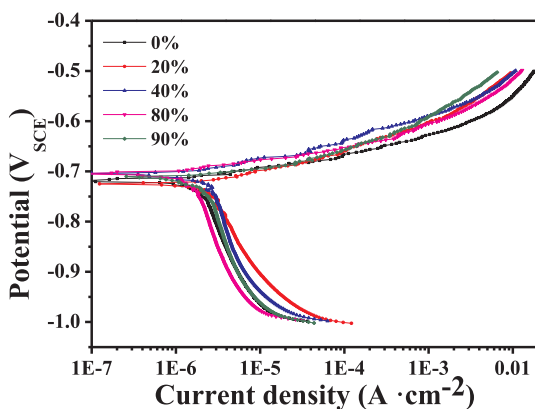

Fig. 5. Potentiodynamic scanning curves of Al-TiB$_2$/TiC composites with different rolling reduction in 3.5 wt.% NaCl solution.

Table 1
E$_{corr}$ and I$_{corr}$ values of the composites derived from the potentiodynamic scanning curves.

Rolling reduction	E$_{corr}$ (vsSCE)/V	I$_{corr}$/(10^{-6} A·cm^{-2})
0	−0.719	468.0
20%	−0.724	4.6
40%	−0.701	79.1
80%	−0.705	11.4
90%	−0.712	231.6

energy dispersive X-ray spectrometer (EDS, Oxford).

Corrosion tests

Corrosion tests were carried out by suspending samples in 3.5 wt.% NaCl solution at room temperatures. Each sample (10 mm × 10 mm × 1 mm) was mechanically polished with SiC abrasive paper up to 1000 grade and then further polished with SiO$_2$ suspension solution. The polished samples were washed and ultrasonically rinsed in distilled water before the further tests. Weight loss test were taken to determine the corrosion rate of Al-TiB$_2$/TiC composites and the samples were immersed in the solution for 2, 4, 7 and 9 days, respectively, according to the GB10124-1988 criteria.

laboratory rolling mill for ~1 mm each pass until to the above given reduction. The samples for microstructure characterization and corrosion tests were cut along the rolling direction-transverse direction (RD-TD). Microstructures of these composites before and after corrosion tests were examined by optical microscope (OM) and a field emission scanning electron microscope (FESEM, Quanta 250F) equipped with an
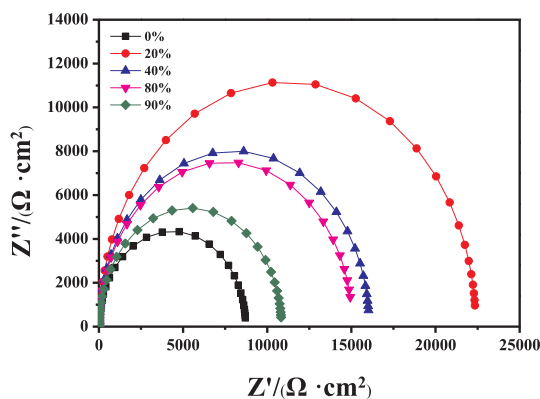
Fig. 6. Electrochemical impedance spectroscopy diagrams for different Al-TiB$_2$/TiC composites after immersion in 3.5 wt.% NaCl solution for 2 h.
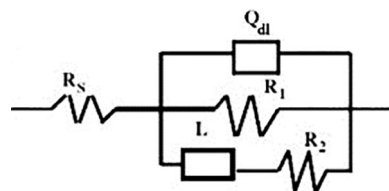

Fig. 7. Equivalent circuit for surface and cross samples of Al-TiB$_2$/TiC composites after hot rolling.

Electrochemical tests were carried out in a conventional three-electrode: a working electrode, a reference electrode (a saturated calomel electrode, SCE) and a counter electrode (platinum sheet) conducted in 3.5 wt.% NaCl solution. Open circuit potential (OCP) values of materials were done for 7200 s and polarization curves were obtained starting from -0.25 V (vs. E$_{corr}$) to $+0.25$ V $_{Ag/AgCl}$ at a scan rate of 1 mV/s. Correspondingly corrosion current density (I$_{corr}$) and corrosion potential (E$_{corr}$) was obtained using the Tafel extrapolation method. Electricity impedance spectrum (EIS) tests were done using a frequency interval of 10^5–0.1 Hz and voltage amplitude of 10 mV. Finally, the SEM images of the surfaces of the Al-TiB$_2$/TiC composites after corrosion tests were obtained to analyze the corrosion mechanism.

Results and discussion

Microstructure of Al-5 wt.% TiB$_2$/TiC composites

Fig. 2 shows the microstructures of Al-5 wt.% TiB$_2$/TiC composite after various rolling reductions. It can be seen that most of TiB$_2$/TiC particles tend to form aggregated clusters [18] and some large particle free zones in the matrix can be seen in Fig. 2a. It is supposed that the bonding between reinforcement and matrix was weak and some micro pores existed in the as-cast microstructure. With the increase of rolling reduction, the reinforcement particles agglomerated in the large clusters were separated with each other to some extent during the deformation. When the reduction increase up to 90%, the original densely gathered particles distributed loosely compared with the as-cast one.

Corrosion behavior of Al-5 wt.% TiB$_2$/TiC composites in 3.5 wt.% NaCl solution

Weight loss

Fig. 3 presents the weight loss of the different samples with respect to duration time in the 3.5 wt.% NaCl solution. It can be seen that weight loss of the samples increases rapidly within the first 4 days and then reached a plateau from 4 to 7 days. However, the weight loss increased rapidly further after 7 days, indicating that the corrosion rate was enhanced with the prolonged holding time. It is noted that the weight loss of the samples after hot rolling treatment is reduced at the same duration time compared with the as-cast one, which suggests that the corrosion resistance of the composites has been improved after the hot rolling treatment. However, with the increase of the rolling reduction from 20% to 90%, the corrosion resistance of the composite is reduced as shown by the weight loss curves in Fig. 3, which indicates that the corrosion resistance is sensitive to the microstructure variation of the composites. Among all the samples, the Al-5 wt.% TiB$_2$/TiC composite with 20% rolling reduction behave the best corrosion resistance. However, it is known that the dislocations in the grains and the sub-grain boundaries increased significantly with the increase of rolling reduction, which is considered to deteriorate the corrosion resistance of the alloy to some extent [25,27]. In our previous work [24], it has been shown that, there are lots of dislocations accumulated in the 90% rolled sample and some dislocation cells formed, both of which lead to the decline of the corrosion resistance. However, compared with the as-cast sample, the rolling treatment with varying strain has improved the corrosion resistance of the composites in different degrees.

In order to investigate the surface morphology of the composites after weight loss tests with different days, the corroded samples were firstly cleaned by CrO$_3$:H$_3$PO$_4$ (specific gravity 1.69) and then the corresponding SEM images were given in Fig. 4. It can be seen from Fig. 4(a), some small and shallow pits with sizes about 10–20 μm formed around the reinforced particles within 2 days, which were TiC and TiB$_2$ particles confirmed by EDS analysis. With the duration time increased to 4 days, the pits size on the surface did not grow obviously as illustrated by Fig. 4(b), while the reinforcements dropped into the solution dramatically, which led to the rapid increase of the weight loss with 4 days consistent with the weight loss trend shown in Fig. 3. Compared with Fig. 4(c) and (b), the size of the pits increased slightly and most of the reinforcement particles dropped, indicating a reduced corrosion rate during this time. However, after 7 days, the isolated pits on the surface connected with each other as shown in the Fig. 4(d) and continuous corrosion channels were formed, which led to the continuous corrosion of the fresh aluminum matrix by Cl$^-$ in the solution. Therefore, the corrosion rate was accelerated further after 7 days.

Electrochemical behavior

Fig. 5 shows the potentiodynamic polarization curves of the Al-5%TiB$_2$/TiC composites in 3.5 wt.% NaCl solution. The current changes smoothly and linearly around the rest potential manifesting cathodic and anodic Tafel behavior. The specific corrosion current density was calculated by Tafel extrapolation for the corrosion potential (E$_{corr}$) and corrosion current density (I$_{corr}$) values, which were shown in the Table 1. It can be seen that the E$_{corr}$ did not change obviously, while the I$_{corr}$ is reduced drastically for the rolled samples compared with that of the as-cast one, which also indicates the corrosion resistance of the composites has been improved. Besides, the sample with 20% reduction with the lowest I$_{corr}$ value behaves the best corrosion resistance compared with others.

Furthermore, the EIS experiments of Al-TiB$_2$/TiC composites with different reduction after immersion in 3.5 wt.% NaCl solution for 2 h were done at the steady-state corrosion potential and the results were shown as Nyquist plots in Fig. 6. Besides, the Equivalent circuit for surface and cross samples of Al-TiB$_2$/TiC composites processed after hot rolling was shown in Fig. 7. Rs is the solution resistance between working and reference electrode, R$_1$ is charge transfer resistance, Q$_{dl}$ is double layer capacitance showing the charge build-up between interface of sample surface and electrolyte, R$_2$ is inductor's resistance and L is inductance in the low frequencies. The radius of the EIS curve (Fig. 6) is in direct proportion to the corrosion resistance of the alloy, the larger of the radius and the better of the corrosion resistance. From Fig. 6, it can be found that Al-TiB$_2$/TiC composites after rolling treatment have better corrosion resistance than the as-cast one. Meanwhile, the corrosion resistance of the composites decreases gradually with the rolling reduction increased from 20% to 90%, which is consist with the weight
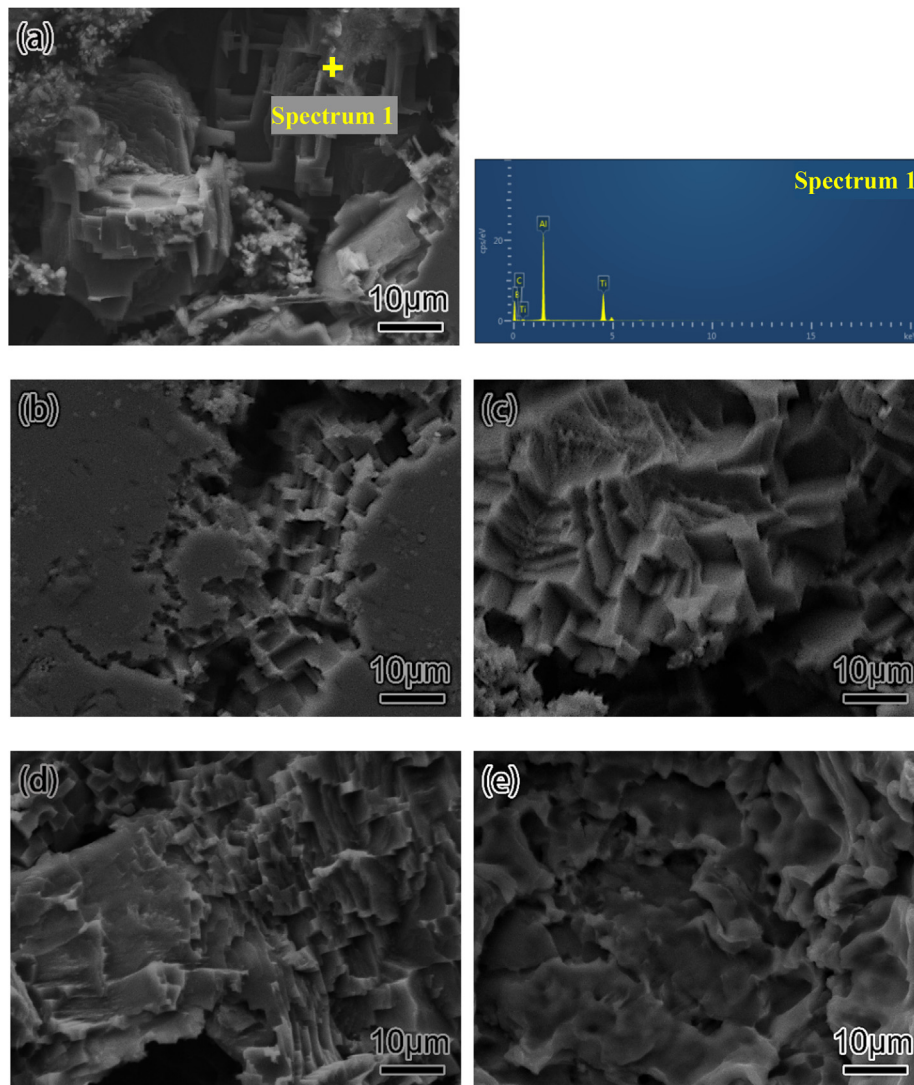
Fig. 8. SEM micrographs of surface morphology after potentiodynamic polarization: (a) as-received; (b) 20%; (c) 40%; (d) 80%; (e) 90%.

loss and potentiodynamic polarization results.

Fig. 8 presented the surface morphologies of the above samples after the electrochemical tests in 3.5 wt.% NaCl solution. It can be seen that a large number of rectangular shallow deep micro-size metastable pits formed on the surface and cover the entire exposed surfaces. Compared with the as-cast one, the size and depth of pits were reduced significantly after rolling treatment, especially after 20% rolling deformation. However, with the reduction increase, the rectangular pits become deeper and the number of corrosion steps increase correspondingly.

Corrosion mechanism of Al-TiB$_2$/TiC composites

To reveal the corrosion mechanism of Al-TiB$_2$/TiC composites, the microstructures of the Al-TiB$_2$/TiC composites with different rolling reduction are shown in the Fig. 9. From the Fig. 9(a), a microvoid can be seen at the interface between the matrix and enforcement particles and then the continuous protective alumina film was broken, which led to the matrix eroded by Cl$^-$ easily in the corrosion environment. After 20% reduction, the microvoids were welded together with the matrix and then the bonding between particles and matrix was better (Fig. 9b), which improved the resistance from the attack of the Cl$^-$. Besides, it has been proved that the dispersive distribution of the reinforced particles in the composites can increase the charge transfer resistance and then improve the pitting corrosion resistance [23,28]. Therefore, the

corrosion resistance of Al-TiB$_2$/TiC composites with 20% reduction has been improved significantly. However, with the increase of the rolling reduction, the dislocations accumulated continuously at the interface of the interfaces between particles and the matrix and then the internal stress concentration formed around the reinforcement particles during the rolling process, which makes the surface of the processed sample more active and thus more susceptible to corrosion attacks [24,25,27].

Based on the above analysis, a schematic is proposed to show the corrosion process of the particle reinforced composites in 3.5 wt.% NaCl solution as shown in Fig. 10. Generally, a protective oxide film formed by the aluminum itself acts as a corrosion resisting layer, which can protect the materials from further corroding when exposed in the corrosion environment. The excellent corrosion resistance of Al and its alloys can be attributed to the compact and continuous oxide film on the surface. However, the protective layer on the surface can be discontinued and weakened by the agglomerated reinforcement particles for Al based composites as shown in Fig. 10a, which leads to the decrease of the corrosion resistance significantly. It has been shown that the sites where these discontinuities occur become the nucleation sites for the corrosion reaction to initiate [29]. It is known that the reinforcement particles have different electrode potential with respect to the Al matrix and a galvanic cell will form between the matrix and the particles, resulting in oxygen reduction [30].Therefore, the interface microstructure is a crucial factor that influencing the corrosion
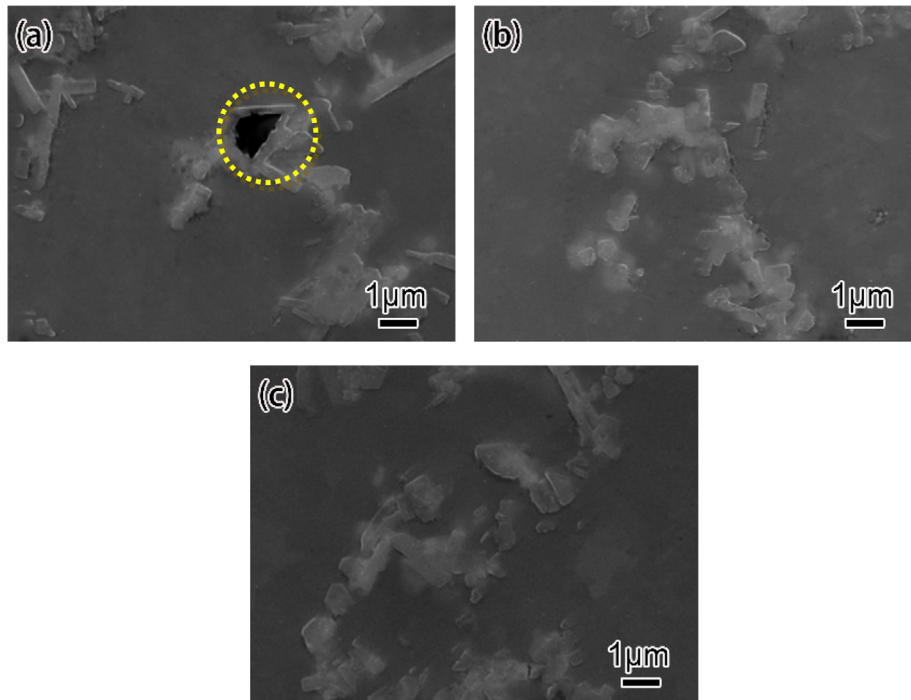
Fig. 9. Microstructures of Al-TiB$_2$/TiC in situ composites with different rolling reduction (in RD-TD plane): (a) 0%; (b) 20%; (c) 80%.
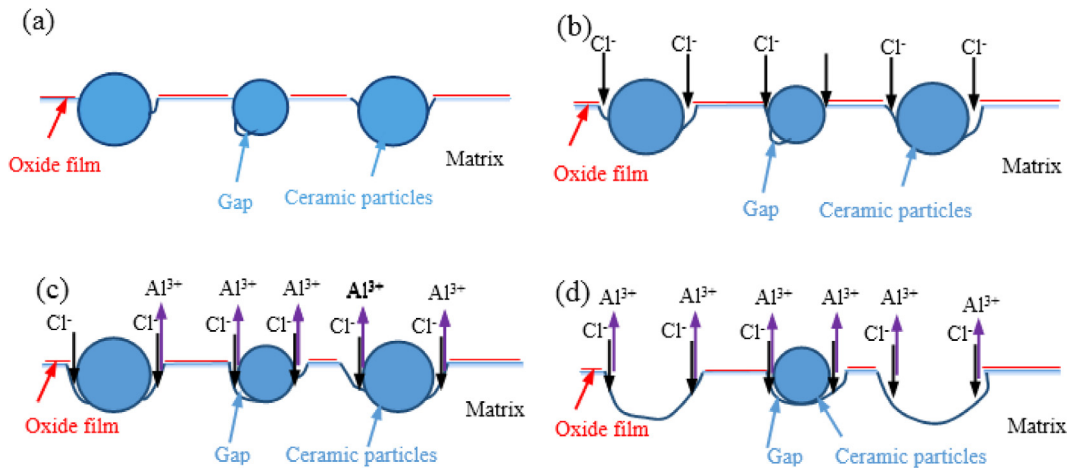

Fig. 10. A schematic for the corrosion mechanism of Al-TiB$_2$/TiC composite in NalCl solution.

resistance of the composites and the existence of microvoids, stress concentration and impurities will reduce the corrosion resistance further. It has been shown that Cl$^-$ in the solvent will accumulate at the microvoids defects and reduce the pH value, which induces the local corrosion i.e. pitting corrosion. Furthermore, it is considered that the reduced oxygen concentration in the microvodis inhibits the reformation of oxide passive film. Therefore, the corrosion of the composites starts from the interfaces with microvoids defects firstly and will extend to the surrounding area forming the large sized corrosion pits. As shown in Fig. 10(b), the Cl$^-$ eroded the interfaces with microvoids defects firstly and led to the anode reaction. With the further proceeding of the corrosion process, oxide film was corroded and then dissolution of Al matrix occurred, along with the reinforced particles falling off from the matrix and then corrosion pits formed as shown in Fig. 10(c, d). Consequently, much more fresh metal surfaces were exposed and then the corrosion pits on the surface grew and connected with each other, which accelerated the corrosion process further.

In the present study, it is found that with a moderate amount of

deformation, the interfaces of the composites will be modified, which is helpful to the improvement of the corrosion resistance. However, the concentration of internal stress at the interfaces of the composites formed during the severely deformation will reduce the corrosion resistance further. The results will provide guidance for the improvement for the corrosion resistance of metal matrix composites reinforced with ceramic particles.

Conclusion

The corrosion behavior of Al-TiB$_2$/TiC composites after hot rolling process was investigated in 3.5 wt.% NaCl solution at room temperature. The results showed that the corrosion of the composites initiated at the interfaces between the Al matrix and the TiB$_2$/TiC particles. During the hot rolling deformation, the particles distribution in the composites has become more and more uniform. According to the weight loss rate, polarization curves and EIS results, the rolling processed Al-TiB$_2$/TiC composites exhibited significant improvement of

corrosion resistance in 3.5 wt.% NaCl solution compared with the as-cast one. Furthermore, the corrosion resistance of the composites was the highest after 20% rolling reduction, which was attributed to the better passive film on the surface due to the enhanced bonding between particles and matrix with less porosity and uniform distribution of enforcement particles. However, with the increase of rolling reduction, the high dislocation density and concentration of internal stress formed in the matrix, which led to the further decrease of the corrosion resistance for the Al-TiB$_2$/TiC composites.

Acknowledgements

Appendix A. Supplementary material

Supplementary data to this article can be found online at https://doi.org/10.1016/j.rinp.2019.102471.

References

[1] Gao Q, Wu S, Shulin LÜ, et al. Improvement of particles distribution of in-situ 5vol% TiB$_2$, particulates reinforced Al-4.5Cu alloy matrix composites with ultrasonic vibration treatment. J Alloys Compd 2017;692:1–9.

[2] Wang F, Xu J, Li J, et al. Fatigue crack initiation and propagation in A356 alloy reinforced with in situ TiB$_2$, particles. Mater Des 2012;33(1):236–41.

[3] Lü L, Lai MO, Su Y, et al. In situ TiB$_2$ reinforced Al alloy composites. Scrip Mater 2001;45(9):1017–23.

[4] Xu J, Zou B, Tao S, et al. Fabrication and properties of Al$_2$O$_3$-TiB$_2$-TiC/Al metal matrix composite coatings by atmospheric plasma spraying of SHS powders. J Alloys Compd 2016;672:251–9.

[5] Fattahi M, Mohammady M, Sajjadi N, et al. Effect of TiC nanoparticles on the microstructure and mechanical properties of gas tungsten arc welded aluminum joints. J Mater Process Technol 2015;217(C):21–9.

[6] Vallauri D, Atías Adrián IC, Chrysanthou A. TiC-TiB$_2$ composites: a review of phase relationships, processing and properties. J Eur Ceram Soc 2008;28(8):1697–713.

[7] Wang H, Wang D, Cheng F, et al. Effect of process conditions on the synthesis of TiB$_2$/TiC nanocomposite powders by mechanical alloying. Rare Metal Mat Eng 2015;44(12):2987–91.

[8] Xiong HH, Zhang HN, Dong JH. Adhesion strength and stability of TiB$_2$/TiC interface in composite coatings by first principles calculation. Comput Mater Sci 2017;127:244–50.

[9] Zhu HG, Min J, Chu D, et al. Study on the reaction mechanism of (α-Al$_2$O$_3$ + TiB$_2$ + TiC)/Al composites fabricated by Al-TiO$_2$-B$_4$C system. Adv Mater Res 2010;150–151:4.

[10] Kim WJ, Yu YJ. The effect of the addition of multiwalled carbon nanotubes on the uniform distribution of TiC nanoparticles in aluminum nanocomposites. Scrip Mater 2014;72–73(2):25–8.

[11] Lakshmi S, Lu L, Gupta M. In situ preparation of TiB$_2$ reinforced Al based composites. Adv Compos Mater 1997;6(4):299–308.

[12] Emamy M, Mahta M, Rasizadeh J. Formation of TiB$_2$ particles during dissolution of TiAl$_3$ in Al-TiB$_2$ metal matrix composite using an in situ technique. Compos Sci Technol 2006;66(7):1063–6.

[13] Sahoo BN, Panigrahi SK. Synthesis, characterization and mechanical properties of in-situ (TiC-TiB2) reinforced magnesium matrix composite. Mater Des 2016;109:300–13.

[14] Alhajeri SN, Al-Fadhalah KJ, Almazrouee AI, et al. Microstructure and microhardness of an Al-6061 metal matrix composite processed by high-pressure torsion. Mater Charact 2016;118:270–8.

[15] Sabirov I, Kolednik O, Pippan R. Homogenization of metal matrix composites by high-pressure torsion. Metall Mater Trans A 2005;36(10):2861–70.

[16] Sabirov I, Kolednik O, Valiev RZ, et al. Equal channel angular pressing of metal matrix composites: effect on particle distribution and fracture toughness. Acta Mater 2005;53(18):4919–30.

[17] Nie JF, Wang F, Li YS, et al. Microstructure and mechanical properties of Al-TiB$_2$/TiC in situ composites improved via hot rolling. Trans Nonfree Metal Soc 2017;27(12):2548–54.

[18] Loto RT, Babalola P. Effect of alumina nano-particle size and weight content on the corrosion resistance of AA1070 aluminum in chloride/sulphate solution. Res Phys 2018;10:731–7.

[19] Abdulstaar M, Mhaede M, Wagner L, et al. Corrosion behaviour of Al 1050 severely deformed by rotary swaging. Mater Des 2014;57(5):325–9.

[20] Song D, Ai-Bin MA, Jiang JH, et al. Improvement of pitting corrosion resistance for Al-Cu alloy in sodium chloride solution through equal-channel angular pressing. Prog Nat Sci 2011;21(4):307–13.

[21] Nejadseyfi O, Shokuhfar A, Dabiri A, et al. Combining equal-channel angular pressing and heat treatment to obtain enhanced corrosion resistance in 6061 aluminum alloy. J Alloys Compd 2015;648:912–8.

[22] Fattah-Alhosseini A, Naseri M, Alemi MH. Corrosion behavior assessment of finely dispersed and highly uniform Al/B$_4$C/SiC hybrid composite fabricated via accumulative roll bonding process. J Manuf Process 2016;22:120–6.

[23] Darmiani E, Danaee I, Golozar MA, et al. Corrosion investigation of Al-SiC nanocomposite fabricated by accumulative roll bonding (ARB) process. J Alloys Compd 2013;552(10):31–9.

[24] Nie J, Fang W, Li Y, et al. Microstructure evolution and mechanical properties of Al-TiB$_2$/TiC in situ aluminum-based composites during accumulative roll bonding (ARB) process. Materials 2017;10(2):109.

[25] Wang X, Nie M, Wang CT, et al. Microhardness and corrosion properties of hypoeutectic Al-7Si alloy processed by high-pressure torsion. Mater Des 2015;83:193–202.

[26] Niroumand B, Toroghinejad MR, Amirkhanlou S, et al. High-strength and highly-uniform composites produced by compocasting and cold rolling processes. Mater Des 2011;32(4):2085–90.

[27] Akiyama E, Zhang ZG, Watanabe Y, Tsuzaki K. Effects of severe plastic deformation on the corrosion behavior of aluminum alloys. J Solid State Electr 2009;13(2):277–82.

[28] Li Z, Li C, Gao Z, et al. Corrosion behavior of Al-Mg$_2$Si alloys with/without addition of Al-P master alloy. Mater Charact 2015;110(3):170–4.

[29] Pardo A, Merino MC, Arrabal R, Viejo F, Carboneras M, Muñoz JA. Influence of Ce surface treatments on corrosion behaviour of A3xx.x/SiCp composites in 3.5wt.% NaCl. Corr Sci 2006;48:3035–48.

[30] Szklarska-Smialowska Z. Pitting corrosion of aluminum. Corr Sci 1999;41:1743–67.